Multi-Level Wind Turbine Inverter to Provide Grid Ancillary Support

Yogesh Patel[*‡], Adel Nasiri[**]

[*]Rockwell Automation, Mequon, USA
[**]Department of Electrical Engineering, Wisconsin-Milwaukee University, Milwaukee, USA
(yppatel@ra.rockwell.com; nasiri@uwm.edu)

[‡]Corresponding Author: Yogesh Patel, E-mail: yppatel@ra.rockwell.com

Received: 25.10.2014 Accepted: 07.11.2014

Abstract- More utility companies now require wind power plants to participate in grid support functions including frequency, voltage and inertia support. However, typical wind turbine generator configurations cannot provide this support. In this paper, a multi-level inverter based wind turbine power conversion system is investigated. The developed inverter interfaces between the DC bus of a wind turbine power conversion system supported by energy storage elements and the grid. Two control techniques are proposed for capacitor-based and battery-based storage systems to provide grid active and reactive power support. Details of control implementation for grid interface, frequency and voltage droop support are presented. Simulation and experimental results are discussed to verify the viability of the proposed system and control techniques.

Keywords—Energy storage, grid support, wind energy.

1. Introduction

Renewable energy systems are increasingly gaining popularity over conventional energy to provide a sizable contribution to electrical energy generation. In particular, wind power has become a substantial share of the total energy generation. According to the American Wind Energy Association (AWEA), U.S. wind industry now totals 60,007 MW of cumulative wind capacity through the end of December 2012. . The U.S wind industry has added over 35% of all new generating capacity in the last 5 years and is on track for higher wind energy penetration. In addition, utility scaled wind turbines (1.5MW-5MW) have become popular because these are highly efficient and generate cost-competitive electricity at power plant scale. At this power level, medium voltage multi-level inverters are well suited to interface with grid. With advancement in silicon technology, the higher voltage self-commutated switching devices are available in market, which enables supporting higher power medium voltage inverters for wind turbines. The utility scaled wind turbine in power systems creates many technical and non-technical challenges that need to be addressed for successful integrations. The main technical issues related to wind energy are its uncertainty, variability and their impacts on stability, reliability and quality of the electric power [1]. In systems with high wind energy penetrations, unlike conventional generations, sudden changes in active and/or reactive power demand cannot be supported by wind energy. This lack of demand support may create unwanted voltage and frequency variations in the grid. In order to overcome this issue, novel control techniques integrated with energy storage systems can be utilized to mitigate wind energy shortcomings. This will enable wind power plants to have active and reactive power control flexibility and participate in grid support functions in terms of frequency and inertia support, reactive power support, Low Voltage Ride Through (LVRT), and power ramp rate support. Recently various grid codes have been imposed on wind power plants for grid support requirements in order to ensure power system stability and reliability for systems with higher penetrations of wind energy.

Several researchers have worked on the concept of providing ancillary supports to the grid for wind energy systems [16]-[20]. Delille et al. investigate the support for grid frequency excursion due to wind and solar energy variations by applying grid level energy storage systems [18]. Ullah et al. present reactive power support for grid by wind turbine inverters during grid low voltage or fault [19]. Fazeli et al. discuss control method for a system including variable generation and energy storage to provide voltage and frequency support to the grid [20]. Vasquez et al. in [16] and Delghavi et al. in [17] present control techniques for grid side inverters operating droop modes. In this paper, grid voltage

and frequency support for a DC distributed wind farm is presented. The system is connected to the grid through medium voltage inverters. Energy storage elements, batteries or ultracapacitors, are placed on the DC side of the system. Frequency and voltage support requirements for different gird codes are discussed and medium voltage inverter topologies are presented. Detailed discussions on frequency and voltage droop control and inverter controls to provided ancillary supports are presented and verified with modeling and experimental results.

2. Frequency and Voltage Regulation Requirements

Several grid codes impose operational frequency ranges for wind power generators as discussed in [3] and [5]. Based on requirements, the wind generators are required to operate continuously between -5% to +5% frequency variations for the most grids. For the frequency variations between +/- 5 to +/- 6%, the wind generators need to operate for limited time duration. This is very wide range in relation to realistic events. It is due to the wide swing of active power supply and demand at any instant. A wind turbine must be able to operate properly within this frequency range. Outside this range, wind power generators need to isolate themselves from the grid. The national grid code recommends low frequency and high frequency support profiles and requirements on primary and secondary responses as shown in Figure 1. Primary response is defined as the automatic increase or decrease in active power output of a generator set in response to a system frequency variation over the period of 0 to 10 seconds from the time of the start of frequency variation and frequency support up to 30 seconds. Secondary response is fully available by 30 seconds from the time of the start of the frequency variation and will be sustainable for at least 30 minutes. The wind energy falls under the intermittent power source and part of the primary response unit [4]. Wind energy with energy storage unit will be able to provide grid support for 30 seconds or more during low or high frequency conditions. The grid imposes some indirect requirement of reactive power consumption by the wind power in terms of power factor as well [3], [5]. Generally, it is in range of 0.95 lagging to 0.95 leading power factor but sometimes it is depends upon the unit rating. In addition to power factor requirements, grid codes require some level of fault ride-through capabilities for the wind generators [2]. The German grid code requires wind power installations to remain connected during voltage sags down to 0% from the rated voltage at the Point of Common Coupling (PCC) for duration of 150 mS. Moreover, during fault, a reactive current injection up to 100% is required. Similar requirement regarding reactive current injection is present in the Spanish grid code. This requirement is relatively difficult to meet by some of the wind turbine concepts due to lack of energy storage system [6-7].

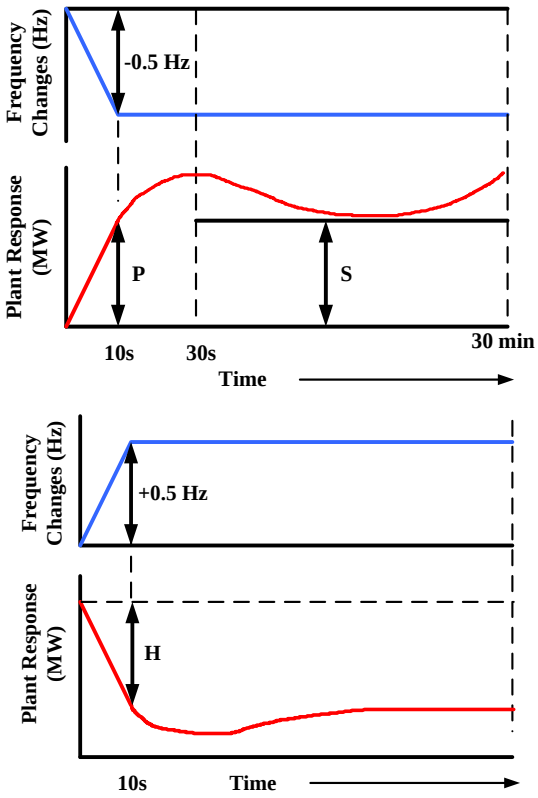

Figure 1. Primary and secondary response requirements of the power generation unit for frequency support during (a) for low frequency conditions, and (b) for high frequency conditions.

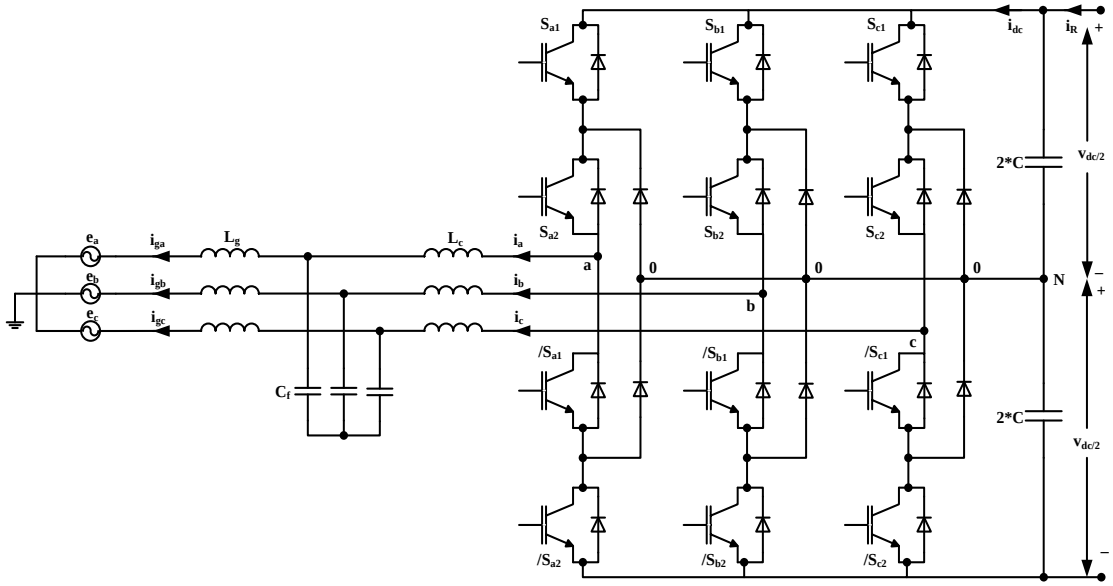

Figure 2. A 3-Level NPC topology for VSC/VSI with LCL filter.

3. Medium Voltage Inverter Topology

The voltage source inverters are classified into two categories: multi-level inverters and high power 2-Level inverters. The multi-level voltage source converters are classified into three different categories namely 3-level neutral point clamp (NPC), cascade H-bridge (CHB) and Flying capacitors. The control for the flying capacitor topology is complex compared with a 3-level NPC converter. In addition, it is more expensive since an excessive number of capacitors are used for voltage clamping and low switching frequency makes these capacitors larger. Disadvantages of the cascade H-bridge converters include need for separate DC sources and a nonstandard transformer [9-10]. The 3-level NPC provides higher quality output voltage and current waveforms and reduced output filter size and cost compared with the two-level inverter. Only half of the DC bus voltage has to be switched and this leads to reduced switching losses. The control loops are also easy to implement. With the availability of IGBT modules of 3.3kV, 4.5kV and 6.6kV rating, 3-Level NPC topology have become very popular for MVDC (2.3kV-4.6kV) applications [8]. The topology of a 3-level NPC is shown in Figure 2. There are four switches per leg. There are also two additional diodes per leg, which link the midpoint of the indirect series connection of the main switches to the neutral point of the converter. This allows the connection of the phase output to the converter neutral point N and enables the three level characteristic of the topology. The two pairs of switches on each leg receive inverted gate signals S_{ak} and $/S_{ak}$ (k=1, 2). Combining the states of all three phases, a 3-level NPC-VSI features total number of switching state equals to $L^3 = 3^3 = 27$, where L is the number of voltage levels of V_{xN} ($x = a, b, c$). Generally, modulation methods used for the 3-level NPC are either carrier based sine-triangular modulation or space vector modulation.

The proposed Multi-level inverter based system to provide grid ancillary support is shown in Figure 3. The power generated by the generator is converted to the DC form using rectifier. The proposed inverter can be used to export from multiple wind turbines sharing a DC bus to the grid. The rectifiers adjust the power from the turbines and can place them on Maximum Power Point Tracking (MPPT). The power is collected from all the turbines and transferred through the grid side inverter. Two energy storage arrangements can be used in this setup. In first arrangement, a battery-based storage system is connected to the shared DC bus through a DC/DC converter, which regulates the DC bus voltage. The inverter can regulate the output active and reactive power in order to provide ancillary services within the capability of the system. The control system must manage the State of Charge (SOC) of the battery simultaneously.

In another arrangement, ultracapacitors (specifically Li-Ion capacitors), which offer high power density, are placed directly on the DC bus to provide energy storage capability [14-15]. In this setup, the DC bus voltage must be variable to provide and receive active power. This will create isolation between input and output power and provide some degree of freedom for inverter active power control in order to provide grid support. The proposed system can perform power ramp rate control, power smoothing, power shifting, and transient stability control.

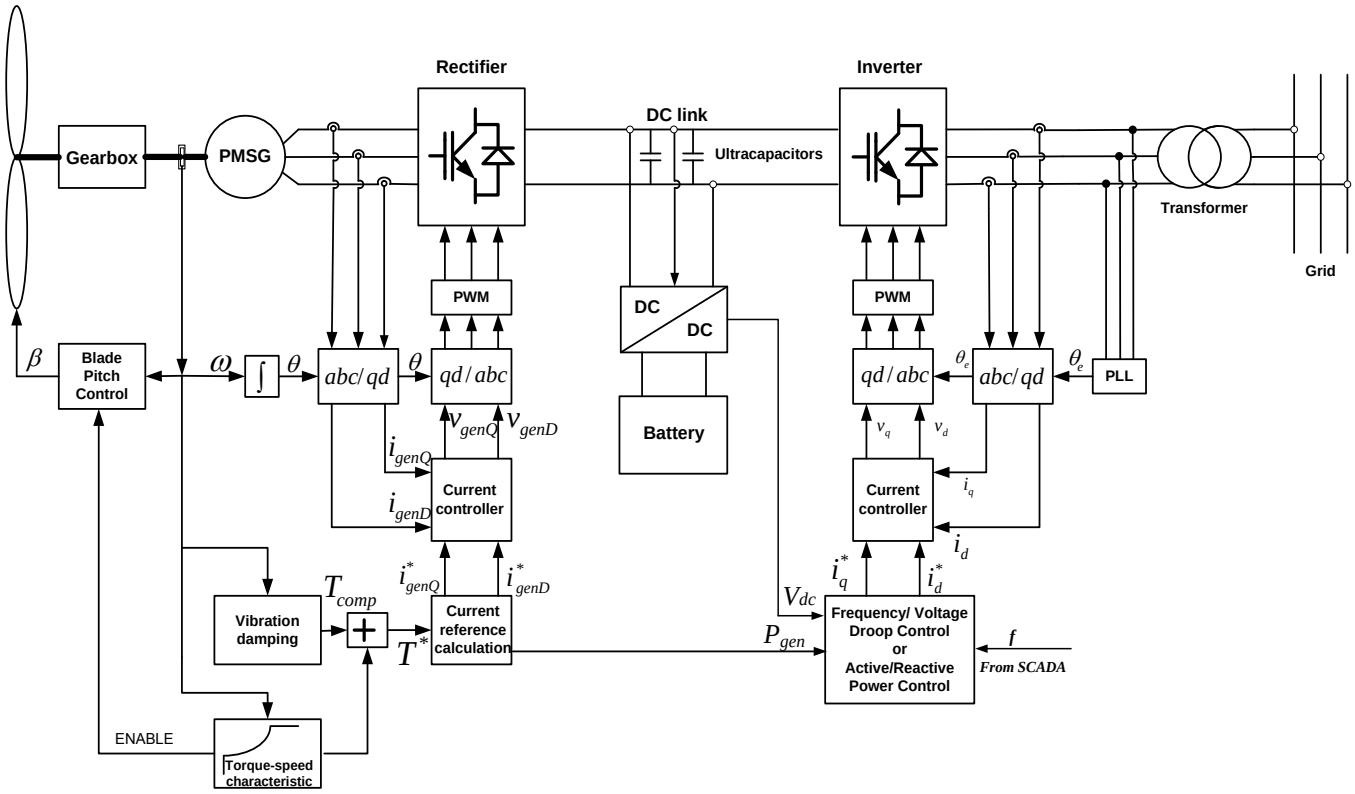

Figure 3. Block diagram of the multi-level inverter systems with frequency and voltage droop support.

4. Frequency and Voltage Droop Control

In order to provide frequency and voltage support to grid we need to establish a relationship between inverter active and reactive power and grid frequency and voltage. A simple two-node system is used here to develop the frequency and voltage droop control equations, which can be extended to a more complex configuration. We consider this two-node system with node 1 as reference with the voltage of $V_1\angle 0$ and node 2 with voltage of $V_2\angle\delta$. The vector diagram of the simplified system is shown in Figure 4. The power flow of the system is given by equations (1) and (2) described below.

$$P = \frac{V_1}{R^2 + X^2}\left(RV_1 - RV_2\cos\delta + XV_2\sin\delta\right) \quad (1)$$

$$Q = \frac{V_1}{R^2 + X^2}\left(XV_1 - XV_2\cos\delta - RV_2\sin\delta\right) \quad (2)$$

For a transmission line, the inductance is much greater than the resistance. Neglecting the resistance R, θ becomes 90˚. Since the power angle δ is typically small, cosδ=1 and sinδ=δ. We can get the following equations.

$$\left(f_1 - f_2\right)t = \frac{\left(P_1 - P_2\right)X}{2\pi V_1 V_2} \quad (3)$$

$$\left(V_1 - V_2\right) = Q\frac{X}{V_1} \quad (4)$$

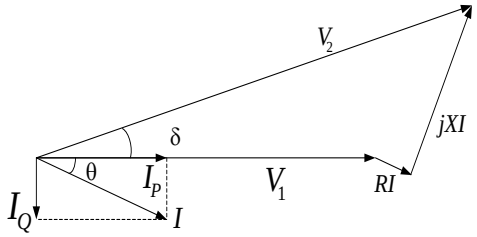

Figure 4. Phasor diagram of currents and voltages for the simplified two-node system.

Frequency susceptibility factor K_{pf} and voltage susceptibility factors K_{qv} can be defined using equations (5) & (6).

$$K_{pf} = \frac{\Delta P}{\Delta f} \quad (5)$$

$$K_{qv} = \frac{\Delta Q}{\Delta V} \quad (6)$$

The grid supply is mostly dominated by synchronous generators, which have an inertial constant described by equation (7).

$$H = \frac{\frac{1}{2}J\omega^2}{MVA} \quad (7)$$

Where H = Inertia constant in MWs / MVA, J is moment of inertia in kgm^2, ω is nominal speed of rotation in rad/s and MVA is the rating of the machine. The majority of generators connected to the grid transmission system have an inertia constant between 3MWs/MVA and 9MWs/MVA. After a system disturbance which results in an imbalance between supply and demand, the inertia prevents an instantaneous change in generator speed and consequently frequency. The rate of change of the speed will be governed by the equation (8) and frequency susceptibility factor K_{Pf} can be defined in term of inertia constant provided by equation (9). Equations (5) through (9) are used to implement the frequency and voltage droop control [11]. Detail inverter control loop is provided in the next section.

$$\Delta f = \frac{\Delta P}{2H} \tag{8}$$

$$K_{pf} = 2H \tag{9}$$

5. Inverter Control

In a typical system, the 3-level NPC VSI in Figure 3 exports active and reactive power to the grid and regulates the DC bus. For all the different control techniques, mathematical model of the balanced three-phase VSI system of Figure 2 can be defined using equation (10), where the filter capacitor is neglected, L represents the total inductance ($L=L_g+L_c$), R represents the total equivalent series resistance of the inductors ($R=R_g+R_c$), and x represent phase a, b and c [12-13].

$$v_x = L\frac{di_x}{dt} + Ri_x + e_x \tag{10}$$

The DC bus voltage regulation is according to equation (11). i_R is the DC output current of the rectifiers and i_{dc} is the input DC current of the inverter.

$$C\frac{dV_{dc}}{dt} = i_R - i_{dc} \tag{11}$$

Applying Clarke and Park transformation and using synchronous reference frame, following equations can be drawn to regulate the inverter output voltage versus direct and quadrature axes currents.

$$v_d = -\left(K_p + \frac{K_i}{s}\right)(i_{dref} + i_d) + \omega L i_q + e_d \tag{12}$$

$$v_q = -\left(K_p + \frac{K_i}{s}\right)(i_{qref} + i_q) - \omega L i_d \tag{13}$$

Equation (11) is converted to equation (14) in control terms to calculate the reference current for d-axis current creating output active power. Q-axis current adjusts the output reactive power as required.

$$i_{dref} \approx i_R - i_{dc} = \left(K_p + \frac{K_i}{s}\right)\left(V_{dc\,ref} - V_{dc}\right) \tag{14}$$

In the system with batteries integrated with the wind turbine at the DC bus through DC/DC converter, both output active and reactive power can be regulated through frequency and voltage droop control methods. The DC bus voltage is regulated by the DC/DC converter. The inverter interfaces with the grid and provides ancillary support using direct active reactive power control techniques. The current parameters in (12)-(13) are replaced by active and reactive power (P and Q) to achieve equations (15)-(16). Detailed block diagram of control loops with direct active/reactive power control for grid ancillary support is shown in Figure 5. Variations in frequency and/or voltage are converted to active and/or reactive power reference commands using PI regulators. Reference for active power is provided based on the support function including inertia or frequency support, power ramp rate support, and power smoothing. The battery State of Charge (SOC) is also regulated at 90% through a slow control loop to allow for both charging and discharging commands.

$$v_d = -\left(K_p + \frac{K_i}{s}\right)(P_{ref} + P) - Q\omega L + e_d \tag{15}$$

$$v_q = \left(K_p + \frac{K_i}{s}\right)(Q_{ref} + Q) - P\omega L \tag{16}$$

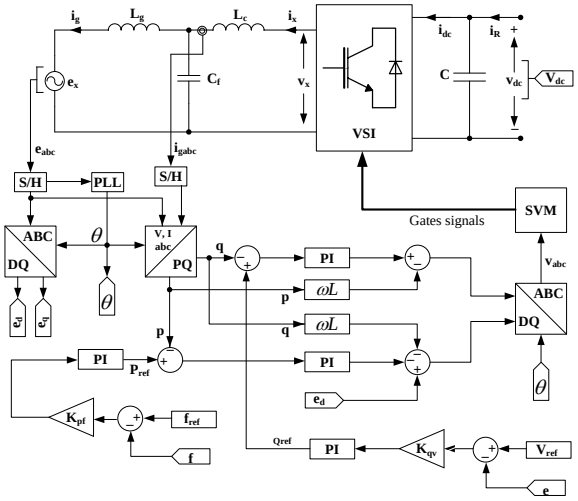

Figure 5.Control block diagram for grid ancillary support based on direct active /reactive power control when using batteries at the DC bus.

In second configuration, ultracapacitors are directly placed on the DC bus. The DC link is supported by the presence of ultracapacitor bank without any DC/DC converter. Therefore, the inverter needs to maintain the DC bus voltage in addition to providing frequency and voltage support to the grid. This is possible by allowing a variable DC bus arrangement to use the energy storage property of ultracapacitors [14-15]. The inverter must keep a minimum DC bus voltage to operate properly. This voltage level is provided by (17).

$$V_{dc\_\min} = \sqrt{2}V_{l-l} * 1.05 \tag{17}$$

The maximum Allowable DC link voltage is governed by the voltage rating of capacitor bank, losses in converter side inductor, rating of the inverter unit and control loop parameters. The energy stored in DC link capacitors is given by equation (18), where P is the power delivered by the capacitor bank. E_{cap} is the energy stored in capacitor in joules.

$$Pt = E_{cap} = \frac{1}{2} C V_{dc}^{\ 2} \tag{18}$$

The maximum energy stored in DC link capacitor bank and available to support grid ancillary services is given by equation (19)

$$\Delta P_{\max} t = E_{cap-\max} = \frac{1}{2} C\left(\Delta V_{dc\_\max}^{\ 2} + 2V_{dc\_\max} V_{dc\_\min}\right) \tag{19}$$

$$\text{Where: } \Delta V_{dc\_\max}^{\ 2} = \left(V_{dc\_\max} - V_{dc\_\min}\right)^2 \tag{20}$$

The total capacitance and ΔV_{dc_max} are selected such that the DC link capacitors can provide frequency support during maximum frequency swing for required duration.

$$2H\Delta f_{\max} t = \frac{1}{2} C\left(\Delta V_{dc\_\max}^{\ 2} + 2V_{dc\_\max} V_{dc\_\min}\right) \tag{21}$$

Using equations (19)-(21), the acceptable variation in DC bus voltage for equivalent frequency variation of Δf can be shown by equation.

$$\Delta V_{dc} = \sqrt{\frac{2K_{pf}\Delta f\ t}{C} - 2V_{dc} V_{dc\_\min}} \tag{22}$$

The block diagram for the control loops with regulated DC bus VSI and frequency and voltage droop support is shown in Figure 6. The differential frequency input is converted to differential DC link voltage using frequency susceptibility factor and other parameters. The differential voltage is added to the actual DC bus voltage and is compared with the min-max DC bus voltage limits. Actual V_{dcref} is used if the voltage does hit the maximum or minimum allowed voltages. The control loop provides frequency support as long as DC bus stays within the min-max V_{dcref} limits.

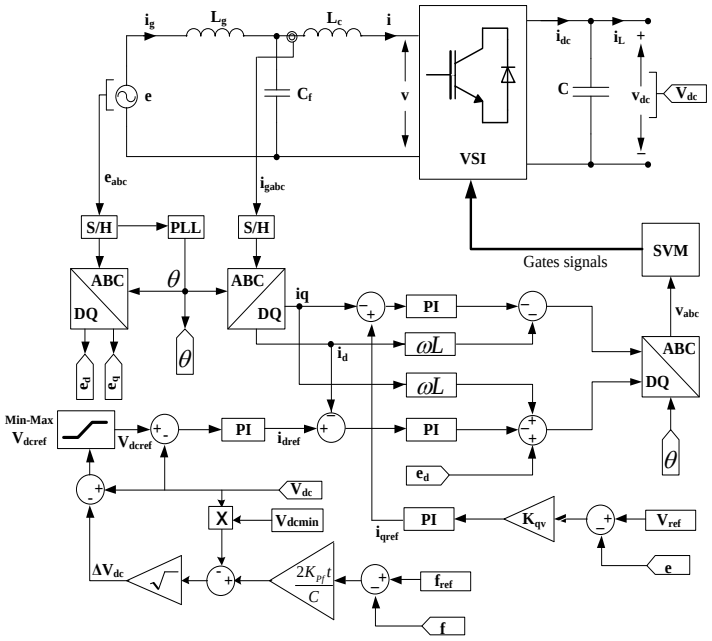

Figure 6. Control loop for Grid ancillary support based on regulated DC bus voltage control when ultra-capacitors are directly connected to the DC bus.

6. Simulation Result

Simulations are performed for a 400Vac, 60Hz, 10kW system with DC bus regulated at 750Vdc. The variable frequency and variable voltage source models are developed in Matlab Simulink environment. When the frequency of the source varies from the nominal value (60Hz), the frequency droop control adjusts active power delivery to the grid to keep the frequency within the limit. Likewise, when voltage amplitude varies from nominal value, the voltage droop control adjusts the capacitive or inductive reactive power to keep the voltage close to the nominal value. The simulation result for frequency droop control is shown in Figure 7. The waveforms from top are phase voltage, line current, reference frequency, actual frequency with and without control, and converter side line to line voltage. One can observe that when the active power demand P_L increases, the frequency droop control injects active power to the grid in order to keep the frequency within acceptable limit define by the grid code. The waveform for the frequency droop control shows that the actual frequency (59.9Hz) is very closely track the reference frequency (60Hz) with control. In absence of the frequency droop control, sudden increase of the active power leads to significant drop in frequency (59.5Hz).

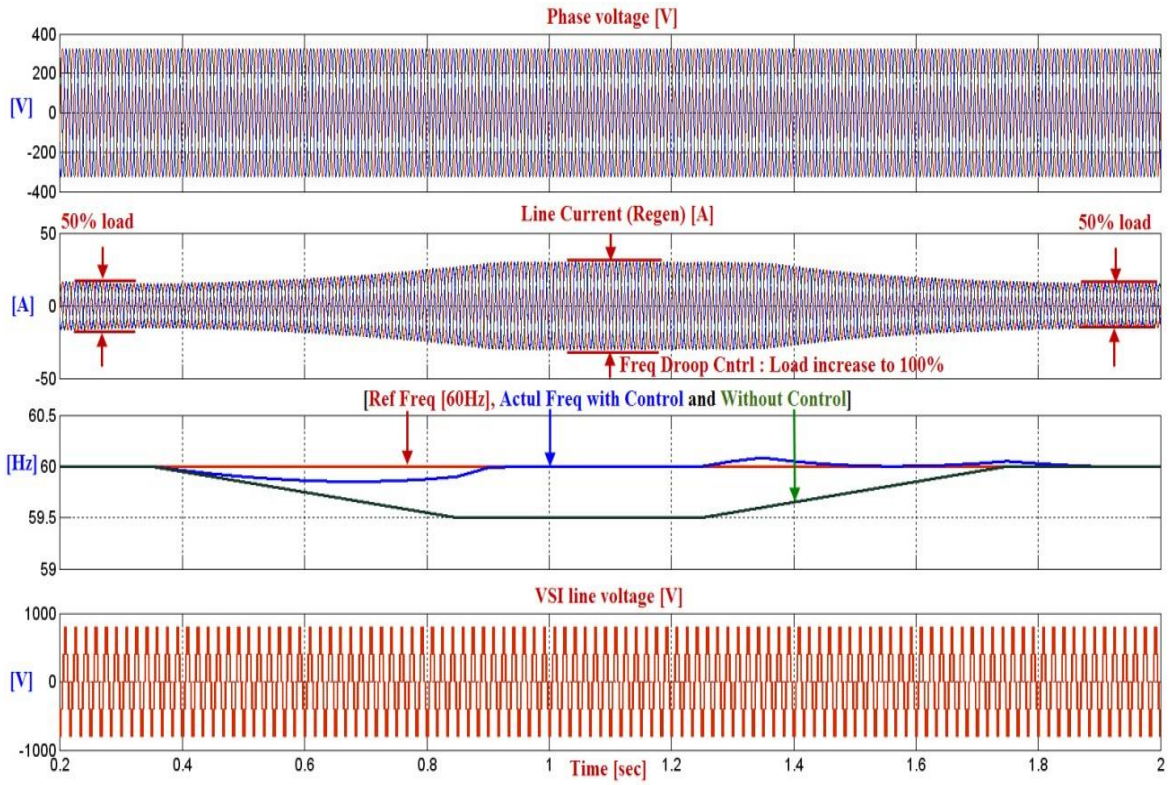

Figure 7. Simulation results for the frequency droop control, (a) three phase voltages , (b) line currents, (c) reference frequency, actual frequency with frequency droop control and frequency without droop control. (d) three phase line voltage at output of voltage source inverter.

Voltage droop control simulation result is shown in Figure 8. The first and second waveforms are the phase voltages with and without voltage support control. The voltage drop with voltage droop control is less than 10% whereas without is about 50%. The third waveform shows the line current of the VSI. It can be easily observed that when the reactive power demand increases, the voltage droop control generate higher reactive power reference command in order to keep the bus voltage within acceptable limit.

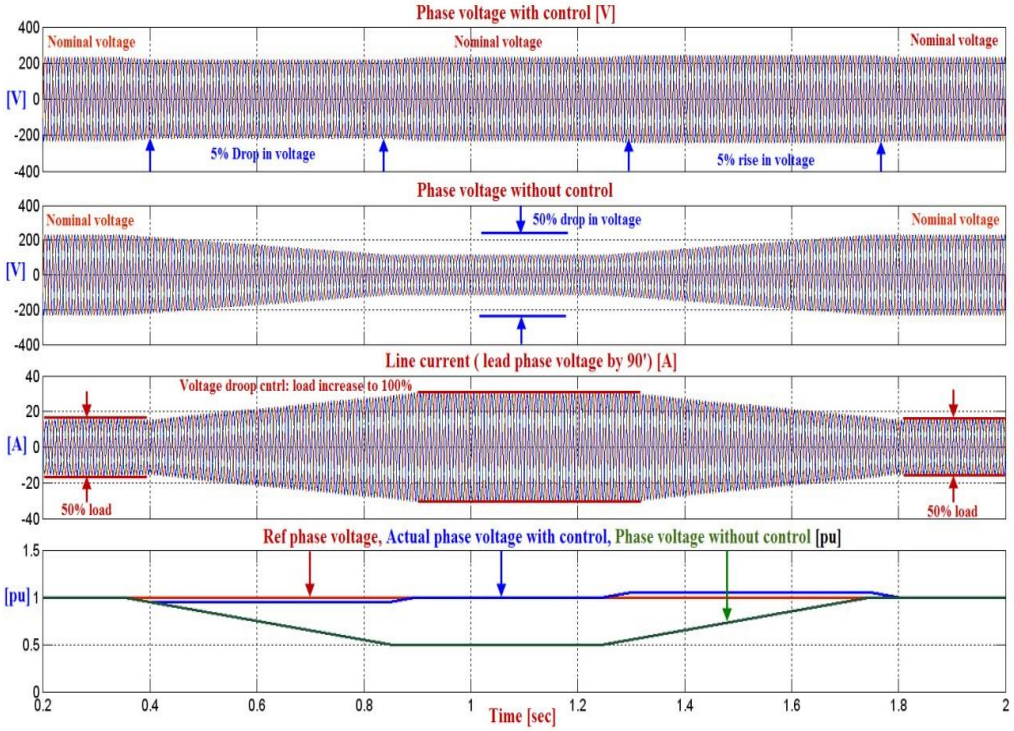

Figure 8. Simulation results for voltage droop control (a) three phase voltages with the voltage droop control , (b) three phase voltages without any voltage droop control implementation, (c) line currents with voltage droop control (d) per unit reference

phase voltage, actual phase voltage with voltage droop control and phase voltage without any implementation of the voltage droop control.

7. Experimental Result

The experimental setup for the frequency and voltage droop control is shown in Figure 9. The setup is rated at 10kW, 400Vac. The active front end based regulated DC bus supply represents the combined system of the energy storage with DC/DC converter and the wind generator. The inverter power structure is connected to the source via an inductor and Δ-Y transformer. The Δ-Y transformer with floating neural is used to avoid common mode circulating current. In order to simplify the experimental setup, only inductor is used instead of an LCL filter. The frequency and voltage droop control is implemented in the controller board of the inverter. For the frequency droop support, the frequency feedback must be provided by the upper level SCADA system of the grid. For the voltage droop support, line voltage is measured by the individual VSI since voltage may vary at various levels of the transmission system.

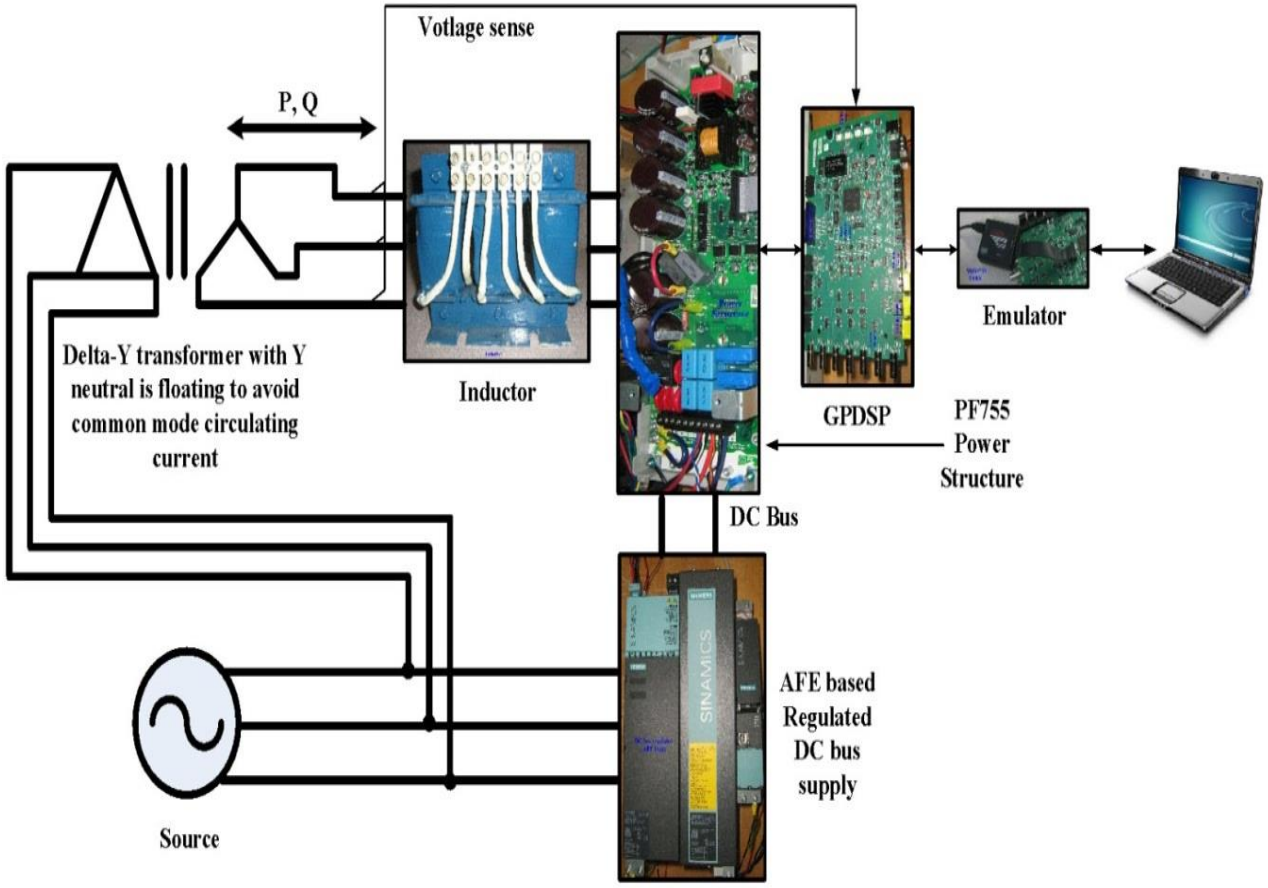

Figure 9. Experimental setup for the frequency and voltage droop control: 400Vac, 10kW rated unit. AFE unit regulated the DC bus and PF755 power structured is controlled using DSP board for frequency and voltage droop control.

The experiment setup was run for both frequency droop control and voltage droop control modes. For frequency droop control, actual and reference frequency commands are provided by Matlab Simulink. The active model is generated in Matlab Simulink which is controlling the actual frequency based on active power demand and active power generation by inverter. As shown in Figure 10, if the frequency drops from 60Hz to 59.25Hz. The equivalent active power reference signal is generated based on actual and reference frequency commands. At nominal frequency (60Hz), the VSI is injecting the 50% (5kW) of active power to the grid. When the frequency drop to 59.25Hz, the active power reference command generated is 1.5pu. The VSI unit is injecting 150% (~15kW) active power to the grid to keep the frequency stable. The zoom in waveforms for line voltage and current are shown in Figure 10 for 150% and 50% loading The line voltage and line current are 30 degree phase shifted.

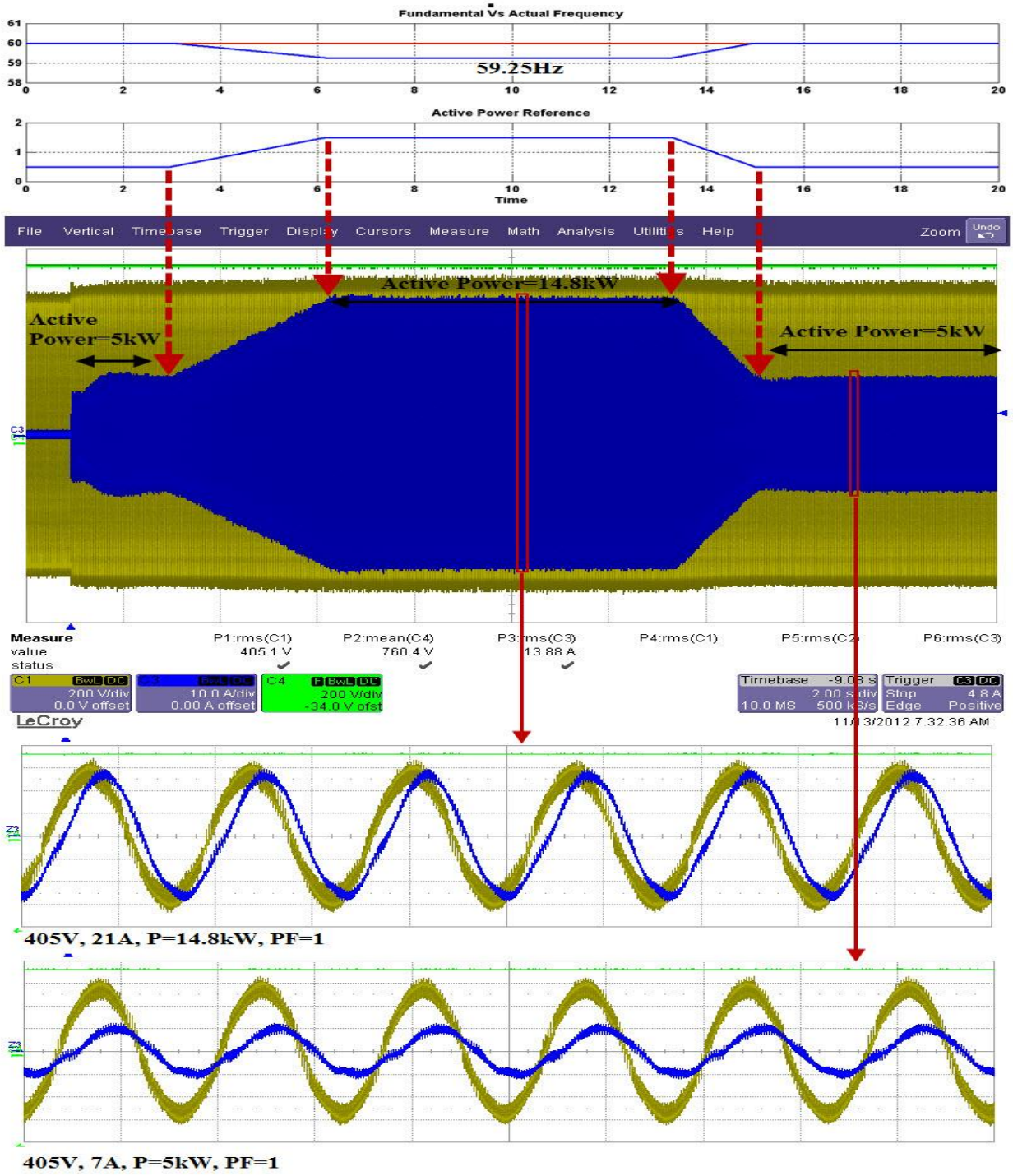

Figure 10. Experimental result for frequency droop support (a) reference frequency, actual frequency and active power reference is generated based on frequency susceptibility factor (b) three phase voltage and current measurement (c) 14.8kW active power delivery during frequency support at unity power factor (d) 5kw active power delivery during nominal frequency condition.

For the voltage droop control, the voltage droop profile is generated in Matlab Simulink environment. The voltage droop profile is shown in figure 11, where the voltage is drop to 60% of the nominal value. The reactive power reference signal is generated and feed to the VSI control. In this case it required 150% reactive power (capacitive) to keep the voltage within limit. The experimental result shows that the VSI control generates the around 120% (12kVAR) reactive power and as the voltage comes back to nominal value it reduces the generation of reactive power gradually up to 50% (4.7kVAR). The zoom in waveforms shows that the line current is leading the phase voltage by 90 degree, which proves that it is running in capacitive reactive power generation mode. Converter side

phase to phase voltage and current waveforms are shown in Figure 12 for the 3-level NPC topology.

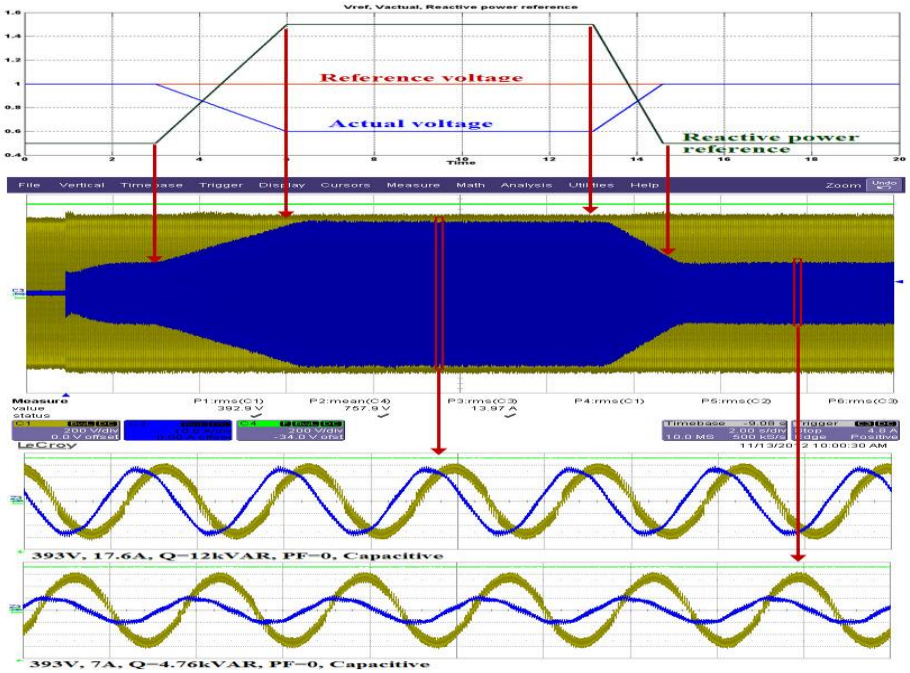

Figure 11. Experimental result for voltage droop support. (a) reference voltage, actual voltage and reactive power reference is generated based on voltage susceptibility factor (b) three phase voltage and current measurement (c) 12kVAR capacitive reactive power delivery during voltage droop support at zero power factor (d) 4.76kVAR reactive power delivery during nominal voltage condition.

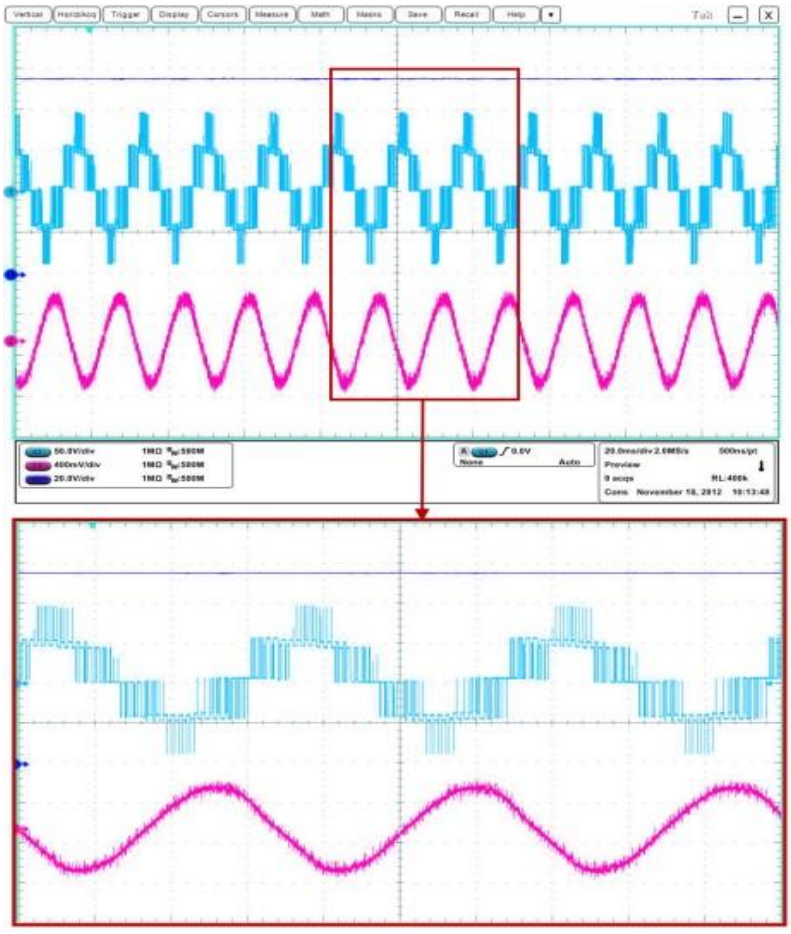

Figure 12. Experimental result of the 3-level NPC inverter with zoom in Line voltage and current

8. Conclusion

In this paper, a multi-level inverter based wind energy conversion system is discussed in details. Energy storage systems have been used at the DC bus in two configurations to provide active power flexibility. The configuration and controls for battery-based and ultracapacitor-based systems have been described. The proposed system applies active and reactive power regulation to support the grid for voltage and frequency droop. Controls for the grid interface and frequency and voltage droop support are presented. Simulation and experimental results of the system are presented to further describe the proposed system.

Acknowledgment

The authors acknowledge the financial support provided for this project under contract MIL104452 by Wisconsin Energy Research Consortium (WERC).

References

[1] M. S. Carmeli, F. Castelli-Dezza, D. Rosati, G. Marchegiani, M. Mauri, "MVDC connection of offshore wind farms to transmission system," *IEEE power electronics electrical drives automation and motion*, pp 1201-1206, 2010

[2] G. Joos, "Wind turbine generator low voltage ride through requirements and solutions" IEEE power and energy general meeting, pp 1-7, 2008

[3] Transmission system interconnection requirements, Manitoba Hydro, Version2, April 2009

[4] Grid code review panel paper: Future frequency response services, National Grid, pp. 10-21, Sep 2010.

[5] M. Tsili, C. Patsiouras, S. Papathanassiou, "Grid code requirements for large wind farms: A review of technical regulation and available wind turbine technology" *IEEE, Renewable power generation IET*, issue 3, pp. 308-332 Sep 2009.

[6] J. P. Barton and D.G. Infield, "Energy storage and its use with intermittent renewable energy," *IEEE Trans. Energy Convers.*, vol. 19, no. 2, pp. 441–448, Jun. 2004.

[7] T. Hennessy and M. Kuntz, "The multiple benefits of integrating electricity storage with wind energy," *IEEE Power Engineering Society General Meeting, 2005.*, vol., no., pp. 1952- 1954 Vol. 2, 12-16 Jun. 2005.

[8] D. Kurg, S. Bernet, S. Fazel, K. Jalili, M. Malinowski, "Comparison of 2.3kV medium voltage multilevel converters for industrial medium voltage drives," *IEEE Trans. Industrial electronics.*, vol. 54, no. 6, pp. 2979–2992, Dec. 2007.

[9] J. Rodriguez, J. S. Lai, and F. Z. Peng, "Multilevel inverter: A survey of topologies, control, and applications," *IEEE Trans. Ind. Electron.*, vol. 49, no. 4, pp. 724–738, Aug. 2002.

[10] J. Rodriguez, S.Bernet, Bin Wu, J.O. Pontt, S. Kouro, "Multilevel voltage- vource-converter topologies for industrial medium-voltage drives," *IEEE Trans.Ind. Appl.*, vol. 54, no. 6, pp. 2930–2945, Dec. 2007

[11] Y. Patel, A. Nasiri, "DC distribution system architecture and control for wind power application," *IEEE Energy conversion congress and exposition (ECCE*)., pp. 3493-3499, Sep 2012.

[12] L. Serpa, S. Ponnaluri, P. Barbosa, J. Kolar, " A modified direct power control strategy allowing the connection of three-phase inverters to the grid though LCL filter," IEEE Transactions on Industrial Applications, vol. 43, no. 5, 2007, Page(s) 1388-1400.

[13] Xu Lie; Zhi Dawei; Yao Liangzhong; "Direct power control of grid connected voltage source converters," *IEEE Power engineering society general meeting*, pp. 1-6, 2007.

[14] A. Esmaili, A. Nasiri, O. Abdel-Baqi, and B. Novakovic, "A Hybrid System of Li-Ion Capacitors and Flow Battery for Dynamic Wind Energy Support," IEEE Transactions on Industry Applications, no. 99, 10.1109/TIA.2013.2255112.

[15] G. Mandic and A. Nasiri "Modeling and Simulation of a Wind Turbine System with Ultracapacitors for Short-Term Power Smoothing," in Proc. IEEE International Symposium on Industrial Electronics, July 2010, Bari, Italy.

[16] C. Vasquez, M. J. Guerrero, A. Luna, P. Rodriguez, R. Teodorescu, "Adaptive Droop Control Applied to Voltage Source Inverters Operating in Grid-Connected and Islanding Modes," IEEE Transactions on Industrial Electronics, vol. 56, no. 10, pp. 4088-4096, 2009.

[17] B. M. Delghavi, A. Yazdani, "An Adaptive Feedforward Compensation for Stability Enhancement in Droop-Controlled Inverter-Based Microgrids," IEEE Transactions on Power Delivery,vol. 26, no. 3, pp. 1764-1773, 2011.

[18] G. Delille, B. Francois, and G. Malarange, "Dynamic Frequency Control Support by Energy Storage to Reduce the Impact of Wind and Solar Generation on Isolated Power System's Inertia," IEEE Transactions on Sustainable Energy, vol. 3, no. 4, pp. 931-939, 2012.

[19] N. R. Ullah, T. Thiringer, and D. Karlsson, "Voltage and Transient Stability Support by Wind Farms Complying With the E.ON Netz Grid Code," IEEE Transactions on Power Systems, vol. 22, no. 4, pp. 1647-1656, 2007.

[20] M. Fazeli, G. Asher, C. Klumpner, and L. Yao, "Novel control scheme for wind generation with energy storage supplying a given demand power," in Proc. 14th International Power Electronics and Motion Control Conference (EPE/PEMC), 2010, pp. S14-15 - S14-21.